J Appl Electrochem (2007) 37:429–438
DOI 10.1007/s10800-006-9257-1

ORIGINAL PAPER

A model for mass transport in the electrolyte membrane of a DMFC

Thomas Vernersson · Göran Lindbergh

Received: 15 August 2005 / Accepted: 5 April 2006 / Published online: 7 February 2007

Abstract A steady state model for multicomponent mass transport was derived for the direct methanol fuel cell membrane. Data for development and validation of the model was taken both from experiments and literature. The experimental data was collected in a polarisation cell, where mass transport of methanol across the electrolyte membrane was measured through a potentiostatic method. The results from modelling and experiments showed good agreement. The model was capable of describing the non-linear response in mass transport to increased methanol feed concentration. The model also accurately described the change in membrane conductivity with methanol concentration. From the model transport equations, it was also possible to derive some characteristic transport parameters, namely the electro osmotic drag of both water and methanol, diffusive drag of water and methanol, and effective, concentration dependent, diffusion coefficients for methanol and water.

Keywords Direct methanol fuel cell · Modelling · Mass transport · Methanol crossover · Electrolyte membrane

List of symbols

a_i	Activity of species “*i*”
c_i	Concentration of species “*i*” [mol m^{-3}]
c_T	Sum of all concentrations [mol m^{-3}]
c_1	Concentration of water [mol m^{-3}]
c_2	Concentration of methanol [mol m^{-3}]
c_3	Concentration of protons [mol m^{-3}]
c_4	Concentration of sulphonic acid groups [mol m^{-3}]
D_{H_2O}	Fickian diffusion coefficient of water [m^2 s^{-1}]
D_{CH_3OH}	Fickian diffusion coefficient of methanol [m^2 s^{-1}]
D_{ij}	Stefan–Maxwell diffusion coefficient of species “*i*” and “*j*” [m^2 s^{-1}]
D_{12}	Stefan–Maxwell diffusion coefficient of water/methanol [m^2 s^{-1}]
D_{13}	Stefan–Maxwell diffusion coefficient of water/proton [m^2 s^{-1}]
D_{14}	Stefan–Maxwell diffusion coefficient of water/sulphonic acid [m^2 s^{-1}]
D_{23}	Stefan–Maxwell diffusion coefficient of methanol/proton [m^2 s^{-1}]
D_{24}	Stefan–Maxwell diffusion coefficient of methanol/sulphonic acid [m^2 s^{-1}]
D_{34}	Stefan–Maxwell diffusion coefficient of proton/sulphonic acid [m^2 s^{-1}]
f_i	Activity factor of species “*i*” [m^3 mol^{-1}]
F	Faraday constant [As mol^{-1}]
$i_{crossover}$	Methanol crossover current [A m^{-2}]
i_{lim}	Limiting current of methanol crossover [A m^{-2}]
i_{load}	Current density load [A m^{-2}]
N_i	Flux of species “*i*” [mol m^{-1} s^{-1}]
N_1	Flux of water [mol m^{-1} s^{-1}]
N_2	Flux of methanol [mol m^{-1} s^{-1}]
N_3	Flux of protons [mol m^{-1} s^{-1}]
R	Gas constant [J mol^{-1} K^{-1}]
T	Temperature [K]
z_i	Electric charge of species “*i*”

T. Vernersson (✉) · G. Lindbergh
Applied Electrochemistry, Chemical Engineering
and Technology, KTH – Royal Institute of Technology,
SE 100 44 Stockholm, Sweden
e-mail: thomasv@ket.kth.se

Greek letters

α_{H_2O}	Electro osmotic drag of water
α_{CH_3OH}	Electro osmotic drag of methanol
α_{H_2O/CH_3OH}	Diffusive drag of water with methanol
α_{CH_3OH/H_2O}	Diffusive drag of methanol with water
ϕ	Potential [V]
η_a	Anodic overpotential [V]
κ	Conductivity [S m^{-1}]
μ_i	Electrochemical potential of species "*i*" [J mol^{-1}]
μ_i^0	Electrochemical potential of species "*i*" at reference state [J mol^{-1}]
v_0	Velocity of reference species [m s^{-1}]
v_j	Velocity of species "*j*" [m s^{-1}]

1 Introduction and theory

1.1 Background

The direct methanol fuel cell (DMFC) is considered a promising and suitable power source for portable electronics. One of the DMFC's main advantages is having a liquid fuel, a water/methanol solution, which carries a high energy density per unit volume and makes fuel handling easier. A liquid fuel also reduces the risk of drying out the electrolyte, which is beneficial since the electrolyte conductivity is dependent on water content. On the other hand, it suffers from a drawback when it comes to performance. The standard potential of the DMFC is 1.21 V (at 25 °C), which is very close to that of the hydrogen/oxygen fuel cell (1.23 V). The cell output voltage is much lower, however, due to a number of factors [1–4]. One of the reasons for the poor DMFC performance is the slow reaction kinetics of methanol oxidation at the anode. The potential loss from anode reaction overpotential at 343 K is estimated to about η_a = 0.2–0.25 V [1]. The reaction kinetics is greatly enhanced by an increase in temperature, but the thermal stability of the membrane limits the operating temperature. An improved electrolyte material or improvements in catalyst structure could reduce this problem. Another problem is the methanol permeability of currently available electrolyte membranes. Methanol crossover to the cathode leads to a mixed potential at this electrode and, as a consequence, to considerable losses in cell potential. The loss in cathode potential from methanol crossover under normal operating conditions has been estimated to be directly proportional to the crossover flow [2]. Methanol crossover also means lower fuel economy, since fuel is lost through the cathode exhaust. The most obvious way of significantly reducing methanol crossover in the fuel cell is to develop membranes that offer good stability and proton conductivity, whilst having low methanol permeability. However, a proton exchange electrolyte will most likely never be completely impermeable to methanol. So even for an improved electrolyte with reduced methanol permeability, there is a need for transport parameter characterisation and optimisation of the cell operating conditions. The transport processes that occur in the electrolyte membrane are hence of great importance. These include methanol and water transport due to concentration gradients across the electrolyte as well as proton conduction and electro osmotic drag, protons moving associated to water and methanol molecules. Much work has been done on characterising the Nafion membrane in a DMFC application with respect to conductivity [5–7], methanol uptake and transport [7–19], and water uptake and transport [14–23]. Some of the findings of other publications, relevant to this work, are gathered in Table 1.

Seeing the importance of mass transport in the electrolyte, methanol crossover is necessarily investigated for new types of membranes in order to appreciate their suitability for use in DMFC. For existing membranes such as Nafion, often used in DMFC research due to the lack of better or cheaper alternatives and because of the extensive characterisation of other properties, the methanol crossover is analysed with the aim of improving performance. Modelling is used to improve the understanding of the mass transport processes that occur and to gain insight in system optimisation with the materials presently used. The modelling work done so far mainly focuses on the transport processes as being of diffusive and convective character, following Fick's law with a correction for the electro osmotic drag [15, 16, 24–33]. However, the findings imply that a strictly linear relation between feed concentration and crossover flow does not describe the transport properly; for example, the change in methanol swelling with methanol concentration [9, 17–19] together with the results obtained by Ren et al. [14].

In this work, a multicomponent model based on concentrated electrolyte theory is therefore proposed. Multicomponent theory offers versatility and a detailed analysis that is not encountered in linear models, and this approach has previously been used to describe mass transport in DMFC electrolyte membranes by Meyers and Newman [34–36] and Weber and Newman [37–39], and also in the H_2/O_2 PEFC electrolyte [40–42].

Table 1 Literature references on water and methanol uptake and transport in Nafion 117

Reference	Investigated parameters/results	Conditions & comments
Verbrugge et al. [5]	D_{H^+} (T) $D_{H^+} = 6.2 \times 10^{-9}\,m^2\,s^{-1}$ (348 K)	Nafion 117 D_{H^+} measured in pure water
Edmondson et al. [6]	κ	Nafion 117 298 K κ measured in pure water and pure methanol
Tricoli et al. [7]	$\kappa(T)$ κ = 0.15 S cm^{-1} (333 K) $D_{CH_3OH}(T)$ $D_{CH_3OH} = 3.4 \times 10^{-10}\,m^2\,s^{-1}$ (333 K)	Nafion 117 D_{CH_3OH} measured in 8% methanol κ measured in pure water
Ramya and Dhathathreyan [9]	$D_{CH_3OH}(c_{CH_3OH})$ Membrane porosity (c_{CH_3OH})	Nafion 115 298 K
Kauranen and Skou [10]	$D_{CH_3OH}(T)$ $D_{CH_3OH} = 5.5 \times 10^{-10}\,m^2\,s^{-1}$ (333 K)	Nafion 117
Ren et al. [14]	κ (T) $D_{CH_3OH}(T)$ $D_{CH_3OH} = 1.2 \times 10^{-10}\,m^2\,s^{-1}$ (343 K)	Nafion 117 Parameters measured in 1 M methanol
Scott et al. [16]	$D_{H_2O}(T) = D_{H_2O,ref}e^{2436(\frac{1}{T_{ref}} - \frac{1}{T})}$ $D_{CH_3OH} = D_{CH_3OH,ref}e^{2436(\frac{1}{T_{ref}} - \frac{1}{T})}$	Nafion 117
Skou et al. [17]	Water uptake Methanol uptake Membrane swelling	Nafion 117 298 K Uptake and swelling measured over methanol mole fraction range 0–1
Ren et al. [18]	Water uptake Methanol uptake Membrane swelling	Nafion 117 295 K Uptake and swelling measured for concentrations c_{CH_3OH} = 0–10 M
Motupally et al. [22]	$D_{H_2O} = 4.17 \times 10^{-4}(1 + 161e^{-\lambda})e^{-\frac{2436}{T}}$	Nafion 117
Ren et al. [23]	$\alpha_{H_2O/H^+}(T)$ $\alpha_{H_2O/H^+} = 3.0$ (343 K)	Nafion 117 Drag measured in 1 M methanol

1.2 Theoretical background and framework

To take into account the coupling in the diffusion fluxes caused by interactions between species, and describe mass transport in the electrolyte without assuming ideal conditions or dilute solution, the Maxwell–Stefan transport equation for concentrated electrolyte theory is used. In this model, the membrane is considered as one homogeneous phase through which all the other species are transported and the gradient in electrochemical potential acts as driving force for mass transport. The one-dimensional transport equation for an isothermal and isobaric system, using the notation of Newman [43], in its general form relates the driving force and the sum of friction forces.

$$c_i \nabla \mu_i = \sum_j M_{ij}(v_j - v_0) \qquad (1)$$

$$\text{where } M_{ij} = \begin{cases} K_{ij} & i \neq j \\ K_{ij} - \sum\limits_k K_{ik} & i = j \end{cases} \quad \text{and} \quad K_{ij} = \frac{c_i c_j RT}{c_T D_{ij}}$$

c_T is the sum of all concentrations and D_{ij} is the Stefan–Maxwell diffusion coefficient that expresses the level of interaction between two species in the concentrated electrolyte. The sum of driving forces must be zero, as stated by the Gibbs–Duhem relation, and this results in three independent equations describing mass transport in a system made up of the four species—water, methanol, protons and sulphonic acid groups ($R{-}SO_3^-$, the polymer backbone). In the transport equations, the frictional interactions between the different species are described through Stefan–Maxwell diffusion coefficients. The movement of the three mobile species, water, methanol, and protons, is expressed in the simplest manner, relative to the velocity of sulphonic acid groups in the membrane backbone $R{-}SO_3^-$, which is zero, since these are immobile.

The electrochemical potential is stated to be the driving force for mass transport in the multicomponent theory. This is defined as

$$\mu_i = \mu_i^0 + RT\ln(a_i) + z_i F\phi \qquad (2)$$

For a neutral species, the third term in the expression, $z_i F\phi$, is zero. Consequently, the electrical state, the potential, is only of interest for one species, namely the protons. Since the choice of reference state is arbitrary [43], the protons are chosen as reference species for defining the potential in the system. Taking the gradient of (2) and combining it with Eq. 1 while assuming that the activity coefficients are independent of concentration, the transport equation is written as

$$\nabla c_i = \sum_j \frac{c_i c_j}{c_T D_{ij}} (v_j - v_0) - \frac{c_i z_i F}{RT} \nabla \phi \tag{3}$$

Seeing that the flux of each species is included through the relation $N_i = c_i v_i$, the equations used to describe mass transport in the membrane can be written out as below. (subindex: $1 = H_2O, 2 = CH_3OH, 3 = H^+, 4 = R{-}SO_3^-$)

$$\nabla c_1 = -\left(\frac{c_2}{D_{12}} + \frac{c_3}{D_{13}} + \frac{c_4}{D_{14}}\right)\frac{N_1}{c_T} + \frac{c_1 N_2}{D_{12} c_T} + \frac{c_1 N_3}{D_{13} c_T} \tag{4}$$

$$\nabla c_2 = \frac{c_2 N_1}{D_{12} c_T} - \left(\frac{c_1}{D_{12}} + \frac{c_3}{D_{23}} + \frac{c_4}{D_{24}}\right)\frac{N_2}{c_T} + \frac{c_2 N_3}{D_{23} c_T} \tag{5}$$

$$\nabla \phi = \frac{RT}{F c_3}\left[\frac{c_3 N_1}{D_{13} c_T} + \frac{c_3 N_2}{D_{23} c_T} - \left(\frac{c_1}{D_{13}} + \frac{c_2}{D_{23}} + \frac{c_4}{D_{34}}\right)\frac{N_3}{c_T} - \nabla c_3\right] \tag{6}$$

1.3 Determining the Stefan–Maxwell diffusion coefficients

To be able to use a multicomponent model, the Stefan–Maxwell diffusion coefficients, D_{ij}, must be known. To determine the D_{ij} used in this model, the transport equations were solved using experimental data of methanol transport through a Nafion 117 membrane. The mass transport data were obtained as explained in the experimental section and presented in the results section. However, the transport equations are modified slightly before they are used for this purpose, and a number of assumptions are made.

1.3.1 Concentration

Solvent uptake and membrane swelling has been examined by other authors in the relevant concentration interval [17–19]. These results were compiled into an empirical linear relation of membrane swelling with solvent uptake, expressing the water concentration as a function of the methanol concentration in the membrane, $c_1 = g(c_2)$ which was used in the calculations together with the electroneutrality condition $c_3 = c_4 = h(c_2)$. Using this together with Eqs. 4 and 5, an expression for water flux is given by

$$N_1 = \frac{\left(\frac{c_1}{\frac{\partial g}{\partial c_2} D_{12}} + \frac{c_1}{D_{12}} + \frac{c_3}{D_{23}} + \frac{c_4}{D_{24}})\right) N_2 + \left(\frac{c_1}{\frac{\partial g}{\partial c_2} D_{13}} - \frac{c_2}{D_{23}}\right) N_3}{\left(\frac{c_2}{D_{12}} + \frac{1}{\frac{\partial g}{\partial c_2}}\left(\frac{c_2}{D_{12}} + \frac{c_3}{D_{13}} + \frac{c_4}{D_{14}}\right)\right)} \tag{7}$$

This expression for the water transport will be valid under the examined conditions, leaving two transport equations with six unknowns. The equation of change for a species "i" is given by

$$\frac{\partial c_i}{\partial t} = -\nabla \cdot N_i + R_i \tag{8}$$

Since calculations are made at steady state and no bulk reactions take place, the fluxes of all species will be constant across the membrane thickness.

1.3.2 Electro osmotic drag of water

The measured electro osmotic drag of water is included as a restriction for the solution. Ren et al. [14, 23] have measured electro osmotic drag and these results were chosen as reference, since the measurements were made in an electrolyte membrane with a methanol concentration of 1 M and at similar operating conditions as those used in this work. Hence, the water transport relative to proton transport was set to $N_{H_2O}/N_{H^+} = 3.0$ at methanol feed concentration 1 M and 343 K.

1.3.3 Diffusion coefficients

Solving the transport equations means fitting six Stefan–Maxwell diffusion coefficients to three equations using three restrictions (boundary concentration, potential drop and water drag) for the solution, so an initial guess is needed of all the Stefan–Maxwell diffusion coefficients. The design of orthogonal experiments to obtain the necessary diffusion coefficient data has been discussed by Bennion and Pintauro [44, 45]. In this work, literature data obtained from similar types of experiments and under the appropriate conditions are used for the starting guess as interaction coefficient. A temperature dependent Fick diffusion coefficient of water and methanol in Nafion was gathered from Scott et al. [16]. Proton diffusion coefficient in Nafion was determined by Dannenberg [42], as was the proton/water diffusion coefficient. Diffusion coefficient of protons in methanol was taken as the self-diffusion coefficient of methanol [46], and the diffusion coefficient of methanol in water was taken from Ref. [47].

1.3.4 Conductivity

The conductivity of the Nafion 117 membrane has been measured in the absence of concentration gradients by Vernersson et al. [48] at 1–8 M methanol concentration. This measured conductivity was compared to the value obtained from the multicomponent model when solving the transport equations and fitting the Stefan–Maxwell diffusion coefficients.

1.3.5 Flat electrode surfaces

Methanol concentration is set to be zero at the permeation cell anode boundary, and equal to the feed concentration at the cathode boundary, i.e. the electrodes are approximated as flat surfaces. In reality, this is not true, since a concentration gradient will be present across the electrode and the anode side methanol concentration will most likely be less than the feed concentration, and at the same time the cathode side concentration will likely be larger than zero. For modelling purposes, treating the electrodes as flat surfaces is considered a good approximation, since the mass transport limitations will be in the electrolyte due to the much higher thickness.

Having incorporated these assumptions into the model, differential equations (5–7) are solved for the measured transport data. The restrictions for the solution are that N_2 and N_3 are given by the limiting current, the boundary concentrations are known and $\nabla \phi$ is calculated from the conductivity and measured current.

2 Experimental

2.1 Method

The transport data used to determine the D_{ij} were obtained from a limiting current method described by Ren et al. [14, 23]. The methanol is fed to a permeation cell, a cell where the anode and the methanol feed channel is located on opposite sides of the membrane. In this configuration the polarisation is controlled and methanol is oxidised after passing through the electrolyte membrane, and hydrogen is produced on the methanol feed side. At a high enough potential, a limiting current is observed that corresponds to the rate of mass transport through the membrane and serves as a measure of the permeability of the electrolyte. Thus, the limiting current is a measure of both the proton and the methanol transport, and the methanol concentration on the electrode surface on both anode and cathode side is known.

2.2 Membrane pre-treatment and cell assembly

The membrane that was used to obtain transport data for the model development and verification was Nafion 117. The membrane was pre-treated by first boiling it in 3% hydrogen peroxide for 1 h, then in milli-Q deionised water for 1 h, and then the membrane was boiled in 0.5 M sulphuric acid for 1 h and finally in milli-Q water again. As anode material, an E-tek developmental gas diffusion electrode for DMFC was used. Pt–Ru (1:1) noble metal loading was 5 mg cm^{-2}. For the cathode, an E-tek Elat electrode with 30% Pt on Vulcan XC-72 was used. Noble metal loading was 0.5 mg cm^{-2}. The electrodes and the membrane were assembled in a 2.25 cm^2 cell, using a clamping pressure of 3 bar.

2.3 Data acquisition

The experiments were carried out at 343 K. Methanol solution was fed to the cathode side of the permeation cell, and nitrogen gas saturated with water was fed to the anode side. The potential of the permeation cell was gradually increased until a limiting current of methanol oxidation on the anode could be observed. The potential was controlled and the current recorded with a PAR 263A potentiostat, and data acquisition was made using Corrware software.

3 Results and discussion

3.1 Experimental results

Results from the limiting current measurements, using methanol feed concentrations in the range 0.1–4.0 M, are displayed, corrected for background current, in Fig. 1. It is noteworthy that the limiting current is not a linear function of methanol feed concentration and hence does not follow Fick's law over the entire range of methanol concentrations, as is assumed in many models of methanol transport [15, 16, 23–32]. The observed curvature in measured data is attributed mainly to the effects of coupling of the fluxes. The activity of methanol in water is fairly constant over the examined concentration interval [49], and the permeation of hydrogen in a fully hydrated Nafion 117 can be neglected.

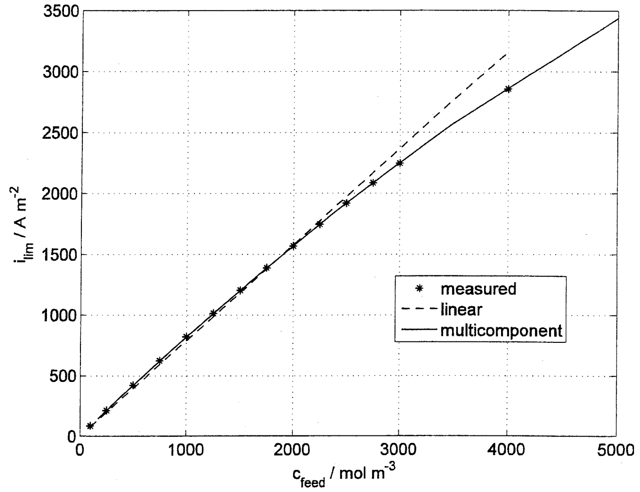

Fig. 1 Measured and calculated limiting current through Nafion 117 at 343 K at different feed concentrations of methanol

3.2 Modelling results

3.2.1 Determining the Stefan–Maxwell diffusion coefficients

The experimental data were used to determine the Stefan–Maxwell diffusion coefficients. As mentioned above, the initial guess for D_{ij} values was based on literature data, obtained under similar conditions as those used in the experimental part of this work. The transport equations were first solved simultaneously for the transport data from each feed concentration separately. Fitting results obtained from these calculations were used as initial guess when solving the transport equations in multiple data points. The resulting Stefan–Maxwell diffusion coefficients, shown in Table 2, were then used to calculate limiting currents in a permeation cell. The accuracy of the multicomponent model was compared to that of a linear model in the examined concentration interval and the result is displayed in Fig. 1. It is evident that the concentrated solution model offers good accuracy and is superior to a linear model over the investigated concentration interval.

The multicomponent theory enables a few characteristic transport parameters to be distinguished from the model results, parameters that are measurable and more informing than merely the Stefan–Maxwell diffusion coefficients when it comes to the understanding of transport processes and system behaviour. These are the electro osmotic drag coefficients, proton conductivity, and apparent Fickian diffusion coefficients. The electro osmotic drag, the number of solute molecules transported with each proton, under fuel cell operation can be defined for both water, α_{H_2O}, and methanol, α_{CH_3OH}. Under conditions of absence of concentration gradients, the following expressions are obtained.

$$\alpha_{H_2O} = \frac{\dfrac{c_1}{D_{13}} + \dfrac{c_1 c_2}{D_{12} D_{23}\left(\frac{c_1}{D_{12}} + \frac{c_3}{D_{23}} + \frac{c_4}{D_{24}}\right)}}{\left(\dfrac{c_2}{D_{12}} + \dfrac{c_3}{D_{13}} + \dfrac{c_4}{D_{14}}\right) - \dfrac{c_1 c_2}{D_{12}^2\left(\frac{c_1}{D_{12}} + \frac{c_3}{D_{23}} + \frac{c_4}{D_{24}}\right)}} \qquad (9)$$

$$\alpha_{CH_3OH} = \frac{\dfrac{c_2}{D_{23}} + \dfrac{c_1 c_2}{D_{12} D_{13}\left(\frac{c_2}{D_{12}} + \frac{c_3}{D_{13}} + \frac{c_4}{D_{14}}\right)}}{\left(\dfrac{c_1}{D_{12}} + \dfrac{c_3}{D_{23}} + \dfrac{c_4}{D_{24}}\right) - \dfrac{c_1 c_2}{D_{12}^2\left(\frac{c_2}{D_{12}} + \frac{c_3}{D_{13}} + \frac{c_4}{D_{14}}\right)}} \qquad (10)$$

The electro osmotic water drag in a membrane equilibrated with pure water was calculated as 2.9, and the electro osmotic methanol drag under conditions of pure methanol was calculated as 0.4. The fact that the model predicts different values of water and methanol drag coefficients is not in line with the notion that the drag is a hydrodynamic flow and that the drag of methanol relative to that of water follows the relative concentration. On the other hand, the relative size of the interaction parameters of water/proton and methanol/proton suggest that the calculated drag should decrease with methanol concentration. The electro osmotic drag of pure methanol was calculated based on Stefan–Maxwell diffusion coefficients fitted at low methanol concentrations, where the system is assumed to be thermodynamically ideal. This value is thus subject to some uncertainty. Calculated values of water and methanol electro osmotic drag in the membrane are displayed in Fig. 2 for a methanol concentration interval where fuel cell operation is plausible and the system is considered thermodynamically ideal. According to the modelling results it appears that total electro osmotic drag is not constant over the entire range of methanol concentration and not even over the smaller concentration interval in which limiting current measurements are performed.

Table 2 Stefan–Maxwell diffusion coefficients at 343 K, fitted in methanol concentration interval 0.5–2.5 M

D_{H_2O/CH_3OH}	D_{H_2O/H^+}	$D_{H_2O/R-SO_3^-}$	D_{CH_3OH/H^+}	$D_{CH_3OH/R-SO_3^-}$	$D_{H^+/R-SO_3^-}$
3.2×10^{-9} m^2 s^{-1}	2.7×10^{-9} m^2 s^{-1}	4.3×10^{-10} m^2 s^{-1}	4.8×10^{-9} m^2 s^{-1}	2.2×10^{-11} m^2 s^{-1}	4.2×10^{-10} m^2 s^{-1}

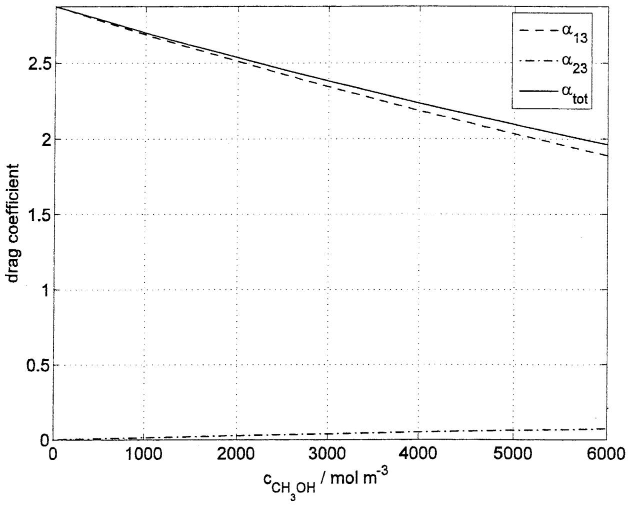

Fig. 2 Electro osmotic drag of water and methanol in the DMFC electrolyte

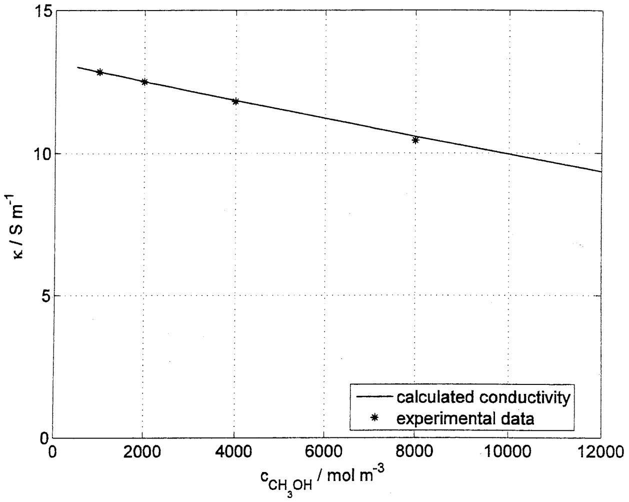

Fig. 3 Conductivity of a fully saturated Nafion 117 membrane at different methanol concentrations. Experimental data and results obtained from the multicomponent model

The diffusive drag of water, the number of water molecules transported with each methanol molecule, α_{H_2O/CH_3OH}, derived from Eq. 4 under open circuit, $\nabla\phi = 0$, and under absence of driving force for diffusion, $\nabla c_1 \rightarrow 0$. Similarly, the diffusive drag of methanol, α_{CH_3OH/H_2O}, is defined from Eq. 5 with $\nabla\phi = 0$ and $\nabla c_2 \rightarrow 0$. The value for the diffusive drag of water with methanol obtained from the model was 5.2 in a membrane saturated with pure water. For methanol with water the diffusive drag was calculated as 1.1 in a membrane saturated with methanol. It is reasonable to think there should be some coefficient linking water and methanol drag, since this too could be thought of as a hydrodynamic transport phenomenon, similar to electro osmotic drag. This could then be interpreted as a measure of the coupling of diffusive fluxes. These coupling effects are the main reason for using the multicomponent transport theory, and they can thus be identified and quantified under special conditions. Instinctively one might expect the diffusive drag coefficients for water and methanol to be of the same magnitude since a Stefan–Maxwell diffusion coefficient exists, expressing to some extent the strength of the interaction between them. However, they also interact with the surrounding polymer membrane, containing both acidic groups and their counter ions. Since these interactions can differ between water and methanol, the diffusive drag may also differ.

The conductivity of the methanol and water filled membrane can be calculated from the transport equations [43]. In this case there is only one charged species carrying the current.

$$\kappa = -F^2 c_3^2 \frac{M_{11}M_{22} - M_{12}^2}{\det(M^0)} \tag{11}$$

M^0 is the transport matrix containing all the elements M_{ij} from Eq. 1. The model corresponds well to the experimental data [48] of conductivity of the methanol and water filled membrane, and the concentration dependence of the conductivity, as shown in Fig. 3. The variation with concentration has not been fully investigated, but Edmondson et al. [6] has reported a decrease in conductivity by one order of magnitude, with a membrane fully saturated with methanol compared to one fully saturated with water. Conductivity calculated using the multicomponent model agrees with values reported by Tricoli et al. [7] and Ren et al. [14], and the decrease is similar in its magnitude to what was reported by Edmondson et al. [6].

Comparing the multicomponent model to a linear model, one can define the measurable, apparent Fickian diffusion coefficient of water or methanol in a membrane of a certain methanol concentration. Using Fick's law together with Eqs. 4 and 5, under open circuit, the following expressions are obtained.

$$D_{H_2O} = -\frac{\left(1 + \dfrac{c_1}{D_{12}\dfrac{\partial g}{\partial c_2}\left(\dfrac{c_1}{D_{12}} + \dfrac{c_3}{D_{23}} + \dfrac{c_4}{D_{24}}\right)}\right)}{\dfrac{c_1 c_2}{D_{12}^2 c_T\left(\dfrac{c_1}{D_{12}} + \dfrac{c_3}{D_{23}} + \dfrac{c_4}{D_{24}}\right)} - \dfrac{\dfrac{c_2}{D_{12}} + \dfrac{c_3}{D_{13}} + \dfrac{c_4}{D_{14}}}{c_T}} \tag{17}$$

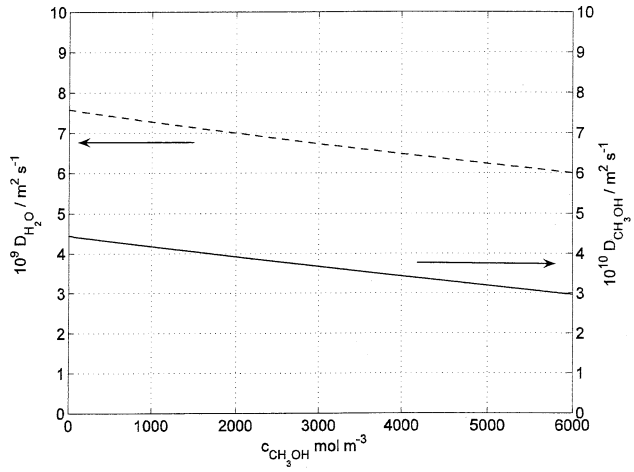

Fig. 4 Modelled Fickian diffusion coefficient of water (upper curve) and methanol (lower curve) in a fully saturated Nafion 117 membrane, at different methanol concentrations

$$D_{CH_3OH} = -\frac{\left(1+\dfrac{c_2\dfrac{\partial g}{\partial c_2}}{D_{12}\left(\dfrac{c_2}{D_{12}}+\dfrac{c_3}{D_{13}}+\dfrac{c_4}{D_{14}}\right)}\right)}{\dfrac{c_1 c_2}{D_{12}^2 c_T\left(\dfrac{c_2}{D_{12}}+\dfrac{c_3}{D_{13}}+\dfrac{c_4}{D_{14}}\right)}-\dfrac{\dfrac{c_1}{D_{12}}+\dfrac{c_3}{D_{23}}+\dfrac{c_4}{D_{24}}}{c_T}} \tag{18}$$

The apparent Fickian diffusion coefficients of water and methanol are displayed as a function of methanol concentration in Fig. 4. Comparing the calculated D_{H_2O} with measured values of the diffusion coefficient of water in Nafion 117 at the relevant temperature, yields mixed results. It is seen that the value calculated using this model differs significantly from the diffusion coefficient published by Scott et al. [16] but is close to that of Verbrugge et al. [5]. Motupally et al. [22] calculated the temperature dependence of the water diffusion coefficient based on the works of three other authors and reached three very different results. The discrepancy in previously published results makes it difficult to evaluate the accuracy of the proposed expression for D_{H_2O}.

The D_{CH_3OH} calculated by the model compares reasonably well with measured values of the diffusion coefficient of methanol at low concentrations. The model predicts a Fickian diffusion coefficient of about 5×10^{-10} m^2 s^{-1} at near zero concentration, which is very close to the value reported by Kauranen and Skou [10]. Ren et al. [14] and Tricoli et al. [7] reported slightly lower values but still in the same order of magnitude. It is notable that the Fickian diffusion coefficients predicted by the multicomponent model are not constant, even at these low concentrations. Looking at the modelling results for higher methanol concentrations, it is seen that the Fickian diffusion coefficient of water continues to decrease, down to a value of about one order of magnitude lower than at conditions of pure water. The Fickian diffusion coefficient of methanol also decreases with increasing methanol concentration, and the behaviour of D_{CH_3OH} at higher methanol concentration seems erroneous at first glance, since it takes a negative value at very high methanol concentrations. However, analogous results have been obtained for different systems through modelling and verified experimentally by Krishna and Wesselingh [50]. The fact that a negative apparent Fickian diffusion coefficient can be observed has to do with the coupling in the diffusion fluxes, and means that the diffusive drag causes one species to be transported against its own concentration gradient, which would normally be the governing driving force for transport. A multicomponent transport model is capable of predicting and handling this behaviour, for which the Fick formulation of mass transport is inadequate. It should be kept in mind however, that at the high methanol concentration where these phenomena seem to occur, no transport data are available to support the model, and thermodynamic non-ideality cannot be assumed, it is merely an extrapolation of the trends shown at lower concentrations.

The fitting of the six Stefan–Maxwell diffusion coefficients reveals that they have a very vague connection to the measured transport data. The fitted Stefan–Maxwell coefficient can deviate from the initial guess by an order of magnitude. This may seem an error in the model, but when analysing the transport equations the actual meaning of the diffusion coefficients becomes apparent. The conclusion is that the measurable diffusion coefficient is a function of concentrations and Stefan–Maxwell diffusion coefficients. This notion is further supported by the fact that the results obtained in this work from fitting the D_{ij} are generally smaller than those obtained by Meyers and Newman [34–36]. Their work was performed at a slightly higher temperature, which can partially explain the difference, but the deviation is not consistent with a similar temperature dependence for all the D_{ij}. The results of Dannenberg [42], obtained using data from a H_2/O_2 PEFC, also differ significantly. All the obtained Stefan–Maxwell diffusion coefficients are reasonable however, as are the calculated transport parameters in the range of methanol concentration where an evaluation can be made. Furthermore, the model predictions of limiting current and membrane conductivities correspond well with experimental data. Examining the sensitivity in the fitting process also implies that there is no real value of the D_{ij}, but what is of greater importance is the magnitude of the D_{ij} values relative to each other. A possible cause for this apparent arbitrariness is the relatively small amount of experimental data used for parameter fitting. As mentioned earlier, more methanol transport data and conductivity data could be added. A reasonable compromise would then be to have a sufficient amount of transport data to ensure convergence while retaining the robustness and functionality of the fitting process. The fact that the water flux is not measured directly, but rather expressed as a function of methanol concentration and flux also reduces the number of data for which to solve the model equations. Other methods of measuring the fluxes could be used that also gives the water flux, for example mass spectrometry, but these methods have proven difficult and unstable as well. One further possibility that would be very helpful in increasing the exactness of the fitting procedure would be to have concentrations profiles measured in situ.

3.2.2 Modelling of DMFC operation

When the fitted D_{ij} were used to simulate DMFC operation, the current density and boundary concentrations were set, and then the flux of water and methanol was calculated. Figure 5 shows the influence of load current on methanol crossover current. The effect of electro osmotic drag becomes apparent at higher concentrations, but the effects are very limited. It should be kept in mind also that in a whole cell model, the boundary conditions could be different, i.e. the methanol concentration at the anode boundary could be lower. Therefore the effects of load current would likely be even less significant. The obtained results coincide well with the measured values of methanol crossover currents of Refs. [11–14]. It is seen in Fig. 6 that for a certain current density, the net water transport will be zero at some specific concentration. This is in accordance with findings by Zawodzinski et al. [20] and Springer et al. [25] that net water transport is much lower than the measured electro osmotic drag due to back diffusion of water from the cathode. These results could also be interesting to consider in conjunction with a cathode model, since flooding of the cathode is a potential problem in the DMFC. Hence, the multicomponent model can offer a valuable tool for describing, analysing, and understanding the important transport processes that occur in the electrolyte membrane.

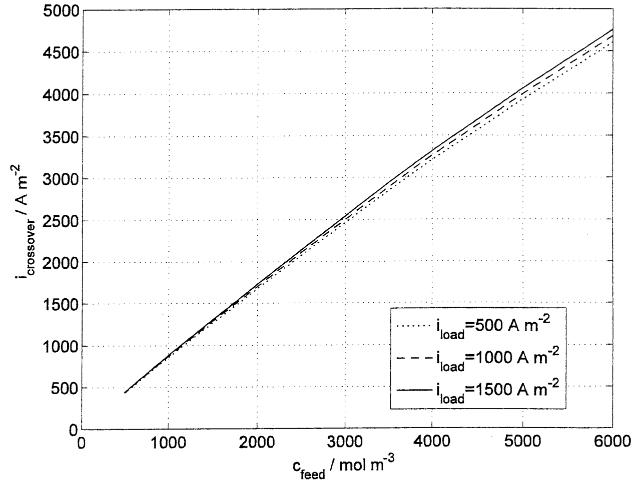

Fig. 5 Methanol flux, expressed as crossover current, through a Nafion 117 electrolyte in a DMFC operating at 343 K, at three different load currents and for different methanol feed concentrations

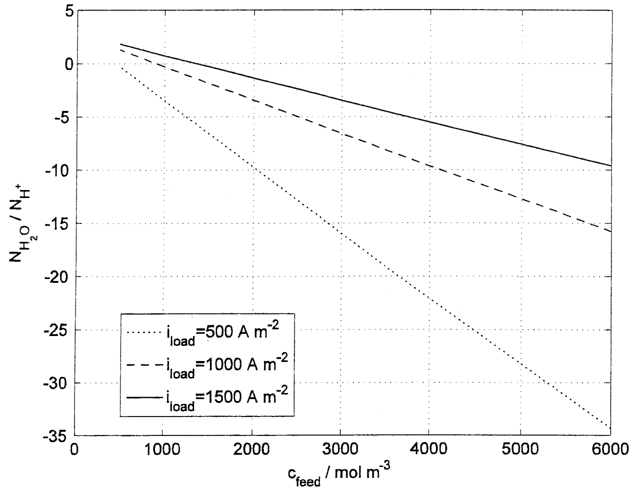

Fig. 6 Net water transport per proton through a Nafion 117 membrane in a DMFC operating at 343 K, at three different load currents and for different methanol feed concentrations

4 Conclusions

Limiting current from methanol transport through a Nafion 117 membrane was measured. The rate of methanol transport through the electrolyte membrane was shown not to obey Fick's law. Significant concentration dependence was observed in the measured limiting current for methanol flux in the permeation cell. A mass transport model based on multicomponent theory was used to describe the mass transport and this model performed well under a wide range of methanol feed concentration. It showed superior capacity to predict permeation flux of methanol through the cell electrolyte compared to a linear model. The model also accurately described the conductivity of the Nafion membrane at different methanol concentrations.

Characteristic transport parameters were derived from the model equations describing some of the transport phenomena in the electrolyte. The coupling in fluxes of water and methanol, the diffusive drag was characterised and expressed as a concentration dependent parameter, as was the electro osmotic drag of both water and methanol. Apparent Fickian diffusion coefficients and the membrane electric conductivity were calculated as functions of concentration and Stefan–Maxwell diffusion coefficients.

The model was also able to predict mass transport of water and methanol at different feed concentrations and under different current load during DMFC operation. An especially interesting feature was that the optimum operating point for maintaining water balance in the DMFC could be determined at given conditions of feed concentration. This is taken as an indication that multicomponent theory is an accurate and versatile tool in DMFC modelling.

Acknowledgements Financing from the Nordic Energy Research Program is gratefully acknowledged. Valuable input from and discussions with Andreas Boden are also acknowledged.

5 Appendix

The linear relation of membrane swelling and solvent uptake was based on data from [17–19]. The swelling and solvent uptake data for the concentration interval 0–10 M, results in the following expressions for water, protons, and sulphonic acid groups.

$$c_1 = g(c_2) = 33455 - 1.3006c_{\mathrm{CH_3OH}}$$

$$c_3 = c_4 = h(c_2) = 1611 - 5.12 \times 10^{-2}c_{\mathrm{CH_3OH}}$$

References

1. Küver A, Vielstich W (1998) J Power Sources 74:211
2. Hikita S, Yamane K, Nakajima Y (2001) JSAE Rev 22:151
3. Gogel V, Frey T, Yongsheng Z, Friedrich KA, Jörissen L, Garche J (2004) J Power Sources 127:172
4. Munichandraiah N, McGrath K, Surya Prakash GK, Aniszfeld R, Olah GA (2003) J Power Sources 117:98
5. Verbrugge MW, Schneider EW, Conell RS, Hill RF (1992) J Electrochem Soc 139:3421
6. Edmondson CA, Stallworth PE, Wintersgill MC, Fontanella JJ, Dai Y, Greenbaum SG (1998) Electrochim Acta 43:1295
7. Tricoli V, Caretta N, Bartolozzi M (2000) J Electrochem Soc 147:1286
8. Barragan VM, Heinzel A (2002) J Power Sources 104:66
9. Ramya K, Dhathathreyan KS (2003) J Electroanal Chem 542:109
10. Kauranen PS, Skou E (1996) J Appl Electrochem 26:909
11. Dohle H, Divisek J, Mergel J, Oetjen HF, Zingler C, Stolten D (2002) J Power Sources 105:274
12. Jiang R, Chu D (2002) J Electrochem Solid State Lett 5:A156
13. Jiang R, Chu D (2004) J Electrochem Soc 151:A69
14. Ren X, Springer TE, Zawodzinski TA, Gottesfeld S (2000) Electrochem Soc 147:466
15. Cruickshank J, Scott K (1998) J Power Sources 70:40
16. Scott K, Taama W, Cruickshank J (1997) J Power Sources 65:159
17. Skou E, Kauranen P, Hentschel J (1997) Solid State Ionics 97:333
18. Ren X, Springer TE, Gottesfeld S (2000) J Electrochem Soc 147:92
19. Thampan T, Malhotra S, Tang H, Datta R (2000) J Electrochem Soc 147:3242
20. Zawodzinski TA Jr, Derouin C, Radzinski S, Sherman RJ, Smith VT, Springer TE, Gottesfeld S (1993) J Electrochem Soc 140:1041
21. Zawodzinski TA Jr, Springer TE, Davey J, Jestel R, Lopez C, Valerio J, Gottesfeld S (1993) J Electrochem Soc 140:1981
22. Motupally S, Becker AJ, Weidner JW (2000) J Electrochem Soc 147:3171
23. Ren X, Henderson W, Gottesfeld S (1997) J Electrochem Soc. 144:L-267
24. Wang ZH, Wang CY (2003) J Electrochem Soc 150:A508
25. Springer TE, Zawodzinski TA, Gottesfeld S (1991) J Electrochem Soc 138:2334
26. Sundmacher K, Scott K (1999) Chem Eng Sci 54:2927
27. Scott K, Argyropoulos P, Sundmacher K (1999) J Electroanal Chem 477:97
28. Divisek J, Fuhrmann J, Gärtner K, Jung R (2003) J Electrochem Soc 150:A811
29. Argyropoulos P, Scott K, Shukla AK, Jackson C (2003) J Power Sources 123:190
30. Kulikovsky AA (2002) Electrochem Commun 4:39
31. Murgia G, Pisani L, Valenti M, Aguanno BD (2002) J Electrochem Soc 149:A31
32. Sandhu SS, Crowther RO, Krishnan SC, Fellner JP (2003) Electrochim Acta 48:2295
33. Murgia G, Pisani L, Shukla AK, Scott K (2003) J Electrochem Soc 150:A1231
34. Meyers JP, Newman J (2002) J Electrochem Soc 149:A710
35. Meyers JP, Newman J (2002) J Electrochem Soc 149:A718
36. Meyers JP, Newman J (2002) J Electrochem Soc 149:A729
37. Weber AZ, Newman J (2003) J Electrochem Soc 150:A1008
38. Weber AZ, Newman J (2004) J Electrochem Soc 151:A311
39. Weber AZ, Newman J (2004) J Electrochem Soc 151:A326
40. Fuller TF, Newman J (1992) J Electrochem Soc 139:1332
41. Janssen GJM (2001) J Electrochem Soc 148:A1313
42. Dannenberg K (2002) Characterisation and modelling of the PEMFC. Ph.D. Thesis, KTH, Stockholm
43. Newman JS (1991) Electrochemical systems, 2nd edn. Prentice Hall, New Jersey
44. Bennion DN, Pintauro PN (1981) AIChE Sympos Ser 77:190
45. Pintauro PN, Bennion DN (1984) Ind Eng Chem Fund 23:230
46. Derlacki ZJ, Easteal AJ, Edge AVJ, Woolf LA, Roksandic Z (1985) J Phys Chem 89:5318
47. Lide DR (ed) (1992) CRC Handbook of Chemistry and Physics, 73rd edn. CRC Press, Ohio
48. Vernersson T, Lafitte B, Lindbergh G, Jannasch P (2006) Fuel Cells 6:340
49. Hu J, Haynes CA, Wu AHY, Cheung CMW, Chen MM, Yee EGM, Ichioka T, Nishikawa K, Westh P, Koga Y (2003) Can J Chem 81:141
50. Krishna R, Wesselingh JA (1997) Chem Eng Sci 52:861